

**DIRECT AND INVERSE SCATTERING OF TIME HARMONIC
ACOUSTIC WAVES IN AN INHOMOGENEOUS
SHALLOW OCEAN**

By

**Yongzhi Xu
T. Craig Poling
and
Trent Brundage**

IMA Preprint Series # 821

June 1991

Direct and Inverse Scattering of Time Harmonic Acoustic Waves in an Inhomogeneous Shallow Ocean

Yongzhi Xu*
Institute for Mathematics and its Applications
University of Minnesota
514 Vincent Hall, 206 Church St. SE
Minneapolis, MN 55455

T. Craig Poling, Trent Brundage
Alliant Techsystems Inc.
600 Second St. NE
Hopkins, MN 55343

I. Introduction

The goal of this research is to develop the theory and a computer simulation to study direct and inverse scattering of time harmonic acoustic waves in inhomogeneous oceans. The present paper will focus on a stratified ocean with a pressure release surface and rigid bottom. A local inhomogeneity (range dependent) is located in the ocean. Our result contains two components:

1. Direct scattering of the incident wave
2. Determination of the inhomogeneity shape from the scattered wave

The direct scattering problem can be formulated as follows: let u^i and u^s be the incident wave and scattered wave, respectively. For a given u^i , we want to solve

$$\nabla^2 u + k^2 n(\mathbf{x}, z) u = 0, \quad -\infty < \mathbf{x} < \infty, \quad 0 \leq z \leq h, \quad (1.1)$$

$$u = 0 \text{ at } z = 0, \quad (1.2)$$

$$\frac{\partial u}{\partial z} = 0, \text{ at } z = h, \quad (1.3)$$

$$u^s(\mathbf{x}, z) \text{ outgoing}, \quad (1.4)$$

where $u = u^i + u^s$ is the total field and the refraction index $n(\mathbf{x}, z)$ has the form of $n(\mathbf{x}, z) = n_0(z)$ for $|\mathbf{x}| > a$. Here n_0 and a are some positive function and constant, respectively. The problem in equations (1.1)-(1.4) will be referred to as Problem 1.

We use a coupled finite element method and normal mode method to produce the propagating waves. There are many publications which address the coupled finite element

* This research was supported in part by the Institute for Mathematics And Its Applications with funds provided by the National Science Foundation, The Minnesota Supercomputer Institute and Alliant Techsystems Inc..

and spectral method. Our method is closest to that in Kirsch and Monk [2]. A brief review of a related method can be found in the introduction of [2].

The inverse scattering problem for acoustic waves, which consists of recovering the inhomogeneity or the shape of the scatterer from the scattered field, forms the basis of a wide variety of areas in the engineering sciences such as remote sensing, nondestructive testing, imaging etc., and for this reason has been the object of study by scientists in a number of diverse disciplines. Recent progress in this field can be found in [1]. However, most of the efforts in this field are devoted to the free space cases of \mathbf{R}^2 and \mathbf{R}^3 . In the homogeneous finite depth ocean, Gilbert and Xu [5] studied the shape determination problem from the "propagating" far-field pattern (ref. [3], [4]). In this paper we will present an algorithm which is a modification of Weston's nonlinear approach [5].

To determine the unknown inhomogeneous medium we make use of the Green's function (denoted by $G(\mathbf{x}, z; \xi, \zeta)$) for the stratified medium to present a relation between the inhomogeneity $m(\mathbf{x}, z) := n(\mathbf{x}, z) - n_0(z)$ and the propagating far-field. Namely, we have

$$u(\mathbf{x}, z) = k^2 \int_{\Omega} G(\mathbf{x}, z; \xi, \zeta) m(\xi, \zeta) u(\xi, \zeta) d\xi d\zeta + u^i(\mathbf{x}, z), \quad (1.5)$$

where $\Omega = \{(\mathbf{x}, z) \mid |\mathbf{x}| < a, 0 \leq z \leq h\}$.

By measuring the scattered wave in the near-field or far-field corresponding to an incident wave, we arrive at solving a minimization problem. This minimization problem is solved by a least-squares algorithm.

II. Coupled Finite Element and Normal Mode Methods for Scattering in an Inhomogeneous Finite Depth Ocean

2.1. Formulation of the Coupled Problem

In this section we study the numerical treatment of the direct scattering in Problem 1. We use the finite element method to approximate u in the neighborhood of the inhomogeneity. Then we match the near-field finite element solution with the far-field normal mode expansion solution by introducing an artificial boundary $\Gamma_a = \{(\mathbf{x}, z) \mid |\mathbf{x}| = a > 0, 0 \leq z \leq h\}$ and domain $\Omega_a = \{(\mathbf{x}, z) \mid |\mathbf{x}| < a, 0 \leq z \leq h\}$. Instead of solving Problem 1, we consider a coupled problem as shown in Figure 2.1. In $\Omega_a = [0, h] \times [-a, a]$, $a > 0$, we consider

$$\Delta u_i + k^2 n(\mathbf{x}, z) u_i = 0, \quad \text{in } \Omega_a, \quad (2.1)$$

$$u_i(\mathbf{x}, 0) = 0, \quad |\mathbf{x}| \leq a, \quad (2.2)$$

$$\frac{\partial u_i}{\partial z}(\mathbf{x}, h) = 0, \quad |\mathbf{x}| \leq a, \quad (2.3)$$

$$\frac{\partial u_i}{\partial |\mathbf{x}|} + i k u_i = \lambda, \quad 0 \leq z \leq h, |\mathbf{x}| = a \quad (2.4)$$

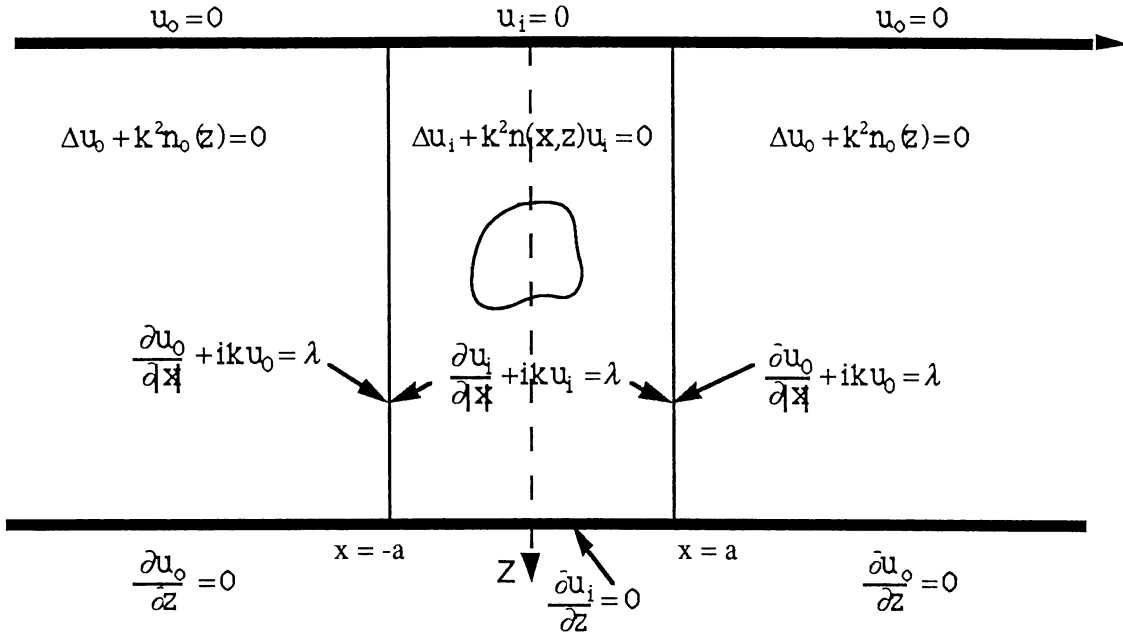


Figure 2.1 Coupling of finite element and normal mode regions.

Equations (2.1)-(2.4) will be referred to as Problem 2. This problem defines an operator G_i :

$$u_i(\mathbf{x}, z) = (G_i \lambda)(\mathbf{x}, z), \quad (\mathbf{x}, z) \in \Omega \quad (2.5)$$

In $\Omega^e = [0, h] \times \{\mathbf{x} \mid |\mathbf{x}| > a\}$, we look for u_0 such that

$$\Delta u_0 + k^2 n_0(z) u_0 = 0, \quad (2.6)$$

$$u_0(\mathbf{x}, 0) = 0, \quad |\mathbf{x}| \geq a, \quad (2.7)$$

$$\frac{\partial u_0}{\partial z}(\mathbf{x}, h) = 0, \quad |\mathbf{x}| \geq a, \quad (2.8)$$

$$\frac{\partial u_0}{\partial |\mathbf{x}|} + i k u_0 = \lambda, \quad 0 \leq z \leq h, \quad |\mathbf{x}| = a \quad (2.9)$$

$$u_0 \text{ is outgoing.} \quad (2.10)$$

Equations (2.6)-(2.10) will be referred to as Problem 3. It defines an operator G_e :

$$u_0(\mathbf{x}, z) = (G_e \lambda)(\mathbf{x}, z). \quad (2.11)$$

We define a function $u(\mathbf{x}, z)$ in $R_b^2 = \{(\mathbf{x}, z) \in R^2 \mid 0 < z < h\}$ by

$$u(\mathbf{x}, z) = \begin{cases} (G_i \lambda)(\mathbf{x}, z) + G_i \left(\frac{\partial u^i}{\partial |\mathbf{x}|} + i k u^i \right)(\mathbf{x}, z), & \text{if } |\mathbf{x}| < a \\ (G_e \lambda)(\mathbf{x}, z) + u^i(\mathbf{x}, z), & \text{if } |\mathbf{x}| > a \end{cases} \quad (2.12)$$

Then $u(\mathbf{x}, z)$ satisfies

$$\Delta u + k^2 n(\mathbf{x}, z) u = 0 \quad \text{in } R_b^2 \setminus \Gamma_a$$

and (1.2)-(1.4).

In order for $u(\mathbf{x}, z)$ to be the solution to Problem 1, we need to choose λ such that $u(\mathbf{x}, z)$ is smooth on $\Gamma_a = \{(\mathbf{x}, z) \mid |\mathbf{x}| = a, 0 \leq z \leq h\}$. From the definition of $u(\mathbf{x}, z)$, we know that $\left(\frac{\partial}{\partial |\mathbf{x}|} + i k \right) u$ is also continuous on Γ_a . If $u(\mathbf{x}, z)$ is continuous on Γ_a , then $\frac{\partial u}{\partial |\mathbf{x}|}$ is continuous on Γ_a . Therefore, $u(\mathbf{x}, z)$ is a solution to Problem 1.

The requirement of $u(\mathbf{x}, z)$ being continuous implies that

$$(G_i - G_e) \lambda = u^i - G_i \left(\frac{\partial u^i}{\partial |\mathbf{x}|} + i k u^i \right) \quad \text{on } \Gamma_a. \quad (2.13)$$

For a given incoming wave u^i , Problem 1 is equivalent to solving (2.13) for λ on Γ_a . The solution to Problem 1 is obtained by substituting λ into (2.12).

The procedure for solving (2.13) is divided into the following four steps:

- (1) Construct the operator G_i by the finite element method
- (2) Construct the operator G_e by normal mode expansion
- (3) Solve (2.13) by seeking a least square solution λ
- (4) Use (2.12) to construct the numerical solution.

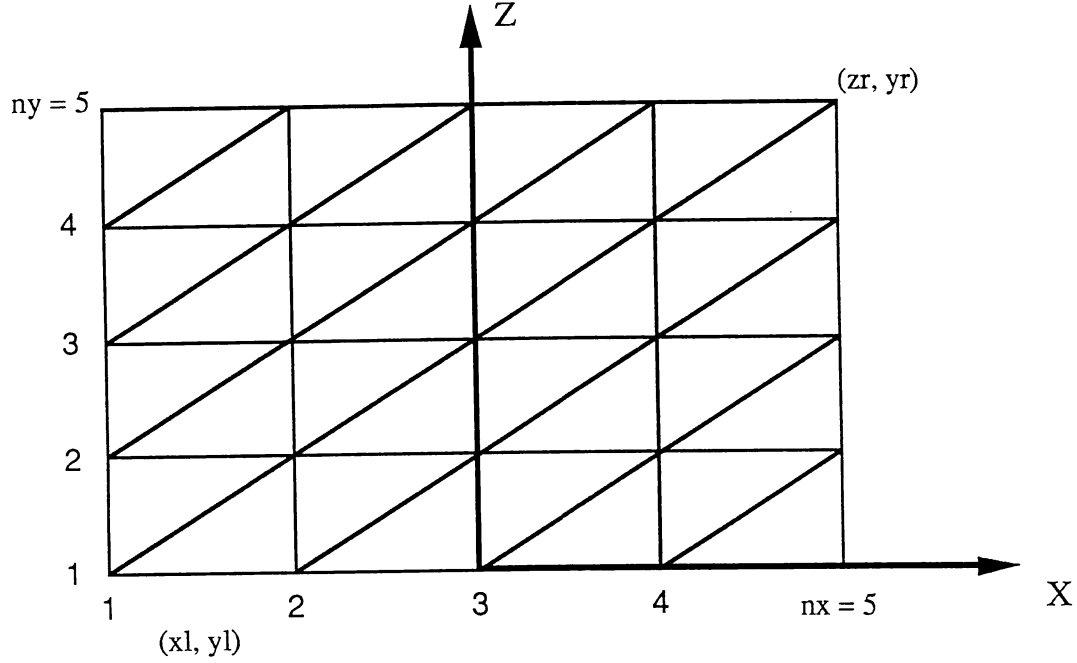


Figure 2.2 Finite element discretization of region containing inhomogeneity.

A more detailed discussion of each step will be presented in the sequel. Numerical test results are presented.

2.2 Algorithm for the Coupled Problem

2.2.1 A Finite Element Algorithm for Problem 2

A standard finite element algorithm is used for solving Problem 2. This algorithm gives the action of the operator G_i acting on a given function λ . We have used a similar algorithm for absorbing boundary conditions as Kirsch and Monk's. The theoretical discussion is omitted, only the numerical scheme is presented.

Approximate Ω by the union Ω_h of linear triangular elements as shown in Figure 2.2.

Let $S_h \subset H^1(\Omega)$ denote the finite element space, $G_i^h \lambda$, the usual finite element solution of Problem 2. Thus G_i is approximated by $G_i^h: H^{-\frac{1}{2}}(\Gamma_a) \rightarrow S_h$ and

$$(\nabla G_i^h \lambda, \nabla \phi_h) - k^2 (n G_i^h \lambda, \phi_h) + ik \langle G_i^h \lambda, \phi_h \rangle - \langle \lambda, \phi_h \rangle = 0$$

for all $\phi_h \in S_h$ and $\lambda \in H^{-\frac{1}{2}}(\Gamma_a)$. Here (\cdot, \cdot) is the inner product in $L^2(\Omega)$ and $\langle \cdot, \cdot \rangle$ is the inner product in $L^2(\Gamma_a)$ or the dual bracket in $\left\langle H^{-\frac{1}{2}}(\Gamma_a), H^{\frac{1}{2}}(\Gamma_a) \right\rangle$.

2.2.2. Normal Mode Expansion Solution for Problem 3

Using a normal mode expansion, we can represent the solution of Problem 3 as

$$\begin{aligned} u_0(\mathbf{x}, z) &= (G_e \lambda)(\mathbf{x}, z) \\ &= \sum_{n=1}^{\infty} \frac{\lambda_n \left(\frac{\mathbf{x}}{|\mathbf{x}|} \right)}{ik(1+a_n)} \phi_n(z) e^{ika_n(|\mathbf{x}|-a)}, \quad |\mathbf{x}| > a, \end{aligned} \quad (2.14)$$

where

$$\lambda(\mathbf{x}, z) = \sum_{n=1}^{\infty} \lambda_n \left(\frac{\mathbf{x}}{|\mathbf{x}|} \right) \phi_n(z), \quad |\mathbf{x}| = a, \quad (2.15)$$

a_n , $\phi_n(z)$ are the n^{th} eigenvalue and normalized eigenfunction for the eigenvalue problem

$$\phi_n''(z) + k^2(n_0^2(z) - a_n^2)\phi_n(z) = 0 \quad (2.16)$$

$$\phi_n'(a) = 0, \quad \phi_n(0) = 0. \quad (2.17)$$

2.2.3. Regularization Solution of (2.13)

Discretizing equation (2.6) by using the finite element solution $G_i^h \lambda_p$ and normal mode expansion solution $G_e \lambda_j$ for $\lambda_j \in M_j := \left\{ f \left| f(\mathbf{x}, z) = \sum_{n=1}^J c_n(\mathbf{x}) \phi_n(z), |\mathbf{x}| = a \right. \right\}$, we obtain a linear system

$$(P_j G_i^h - G_e) \lambda_j = P_j \left(u^i - G_i^h \left(\frac{\partial u^i}{\partial |\mathbf{x}|} + iku^i \right) \right), \quad \text{on } \Gamma_a, \quad (2.18)$$

where P_j is the projection from $C(\Gamma_a)$ to M_j . We then approximate the solution of Problem 1 by

$$u_j^h(\mathbf{x}, z) = \begin{cases} G_i^h \lambda_j^h(\mathbf{x}, z) + G_i^h \left(\frac{\partial u^i}{\partial |\mathbf{x}|} + iku^i \right)(\mathbf{x}, z), & \text{if } |\mathbf{x}| < a, \\ G_e \lambda_j^h(\mathbf{x}, z) + u^i(\mathbf{x}, z), & \text{if } |\mathbf{x}| > a. \end{cases} \quad (2.19)$$

Observe that the corresponding homogeneous equation of (2.18) may have a non-trivial solution, unlike the case discussed by Kirsch and Monk [2]. In fact, for $u^i = 0$, Problem

2.2.2. Normal Mode Expansion Solution for Problem 3

Using a normal mode expansion, we can represent the solution of Problem 3 as

$$\begin{aligned} u_0(\mathbf{x}, z) &= (G_\epsilon \lambda)(\mathbf{x}, z) \\ &= \sum_{n=1}^{\infty} \frac{\lambda_n \left(\frac{\mathbf{x}}{|\mathbf{x}|} \right)}{ik(1+a_n)} \phi_n(z) e^{ik a_n (|\mathbf{x}|-a)}, \quad |\mathbf{x}| > a, \end{aligned} \quad (2.14)$$

where

$$\lambda(\mathbf{x}, z) = \sum_{n=1}^{\infty} \lambda_n \left(\frac{\mathbf{x}}{|\mathbf{x}|} \right) \phi_n(z), \quad |\mathbf{x}| = a, \quad (2.15)$$

a_n , $\phi_n(z)$ are the n^{th} eigenvalue and normalized eigenfunction for the eigenvalue problem

$$\phi_n''(z) + k^2(n_0^2(z) - a_n^2)\phi_n(z) = 0 \quad (2.16)$$

$$\phi_n'(0) = 0, \quad \phi_n(0) = 0. \quad (2.17)$$

2.2.3. Regularization Solution of (2.13)

Discretizing equation (2.6) by using the finite element solution $G_i^h \lambda_p$ and normal mode expansion solution $G_\epsilon \lambda_j$ for $\lambda_j \in M_J := \left\{ f \left| f(\mathbf{x}, z) = \sum_{n=1}^J c_n(\mathbf{x}) \phi_n(z), |\mathbf{x}| = a \right. \right\}$, we obtain a linear system

$$(P_J G_i^h - G_\epsilon) \lambda_j = P_J \left(u^i - G_i^h \left(\frac{\partial u^i}{\partial |\mathbf{x}|} + ik u^i \right) \right), \quad \text{on } \Gamma_a, \quad (2.18)$$

where P_J is the projection from $C(\Gamma_a)$ to M_J . We then approximate the solution of Problem 1 by

$$u_j^h(\mathbf{x}, z) = \begin{cases} G_i^h \lambda_j^h(\mathbf{x}, z) + G_i^h \left(\frac{\partial u^i}{\partial |\mathbf{x}|} + ik u^i \right)(\mathbf{x}, z), & \text{if } |\mathbf{x}| < a, \\ G_\epsilon \lambda_j^h(\mathbf{x}, z) + u^i(\mathbf{x}, z), & \text{if } |\mathbf{x}| > a. \end{cases} \quad (2.19)$$

Observe that the corresponding homogeneous equation of (2.18) may have a non-trivial solution, unlike the case discussed by Kirsch and Monk [2]. In fact, for $u^i = 0$, Problem

1 may have non-trivial solutions. For example, let $n(\mathbf{x}, z) = n_0^2$ for $|\mathbf{x}| < 1$, $n(\mathbf{x}, z) = 1$ for $|\mathbf{x}| > 1$, Problem 1 has the non-trivial solution

$$u(\mathbf{x}, z) = \begin{cases} a_1 e^{\alpha z} \phi_n(z) & \mathbf{x} < -1 \\ (a_2 e^{i\beta z} + a_3 e^{-i\beta z}) \phi_n(z) & |\mathbf{x}| < 1 \\ a_4 e^{-\alpha z} \phi_n(z) & \mathbf{x} > 1 \end{cases} \quad (2.20)$$

where n is an integer such that $k^2 = \left(n - \frac{1}{2}\right)^2 \pi^2 - \alpha^2 > 0$ and

$n_0^2 = \frac{\left[\left(n - \frac{1}{2}\right)^2 \pi^2 + \beta^2\right]}{k^2}$, $\alpha = \beta \cot \beta$ for given $\beta > 0$. In order to avoid the problem caused by the zero eigenvalue, we look for the solution to the regularized problem

$$\min_{\lambda \in M_j} \left\{ \left\| \left(P_J G_i^h - G_e \right) \lambda - P_J \left(u^i - G_i^h \left(\frac{\partial u^i}{\partial |\mathbf{x}|} + i k u^i \right) \right) \right\| + \varepsilon \|\lambda\|^2 \right\}, \quad (2.21)$$

where ε is a small positive number.

2.3 Numerical Experiments

The code, based on the algorithm above was tested on two examples with known exact solutions. The results are presented below.

Test Example 1.

$$n(\mathbf{x}, z) = \begin{cases} 2 & \text{for } |\mathbf{x}| \leq 0.01, 0 \leq z \leq 1 \\ 1 & \text{for } |\mathbf{x}| > 0.01, 0 \leq z \leq 1 \end{cases}$$

$$u^i(\mathbf{x}, z) = \sin[1.5 \pi z] e^{i k a_2 z}$$

where

$$k = 26.5, a_2 = \sqrt{1 - \frac{1.5^2 \pi^2}{k^2}}$$

Analytic scattered solution:

$$u_e^s(\mathbf{x}, z) = \sin[1.5 \pi z] \cdot u_2^s(\mathbf{x}),$$

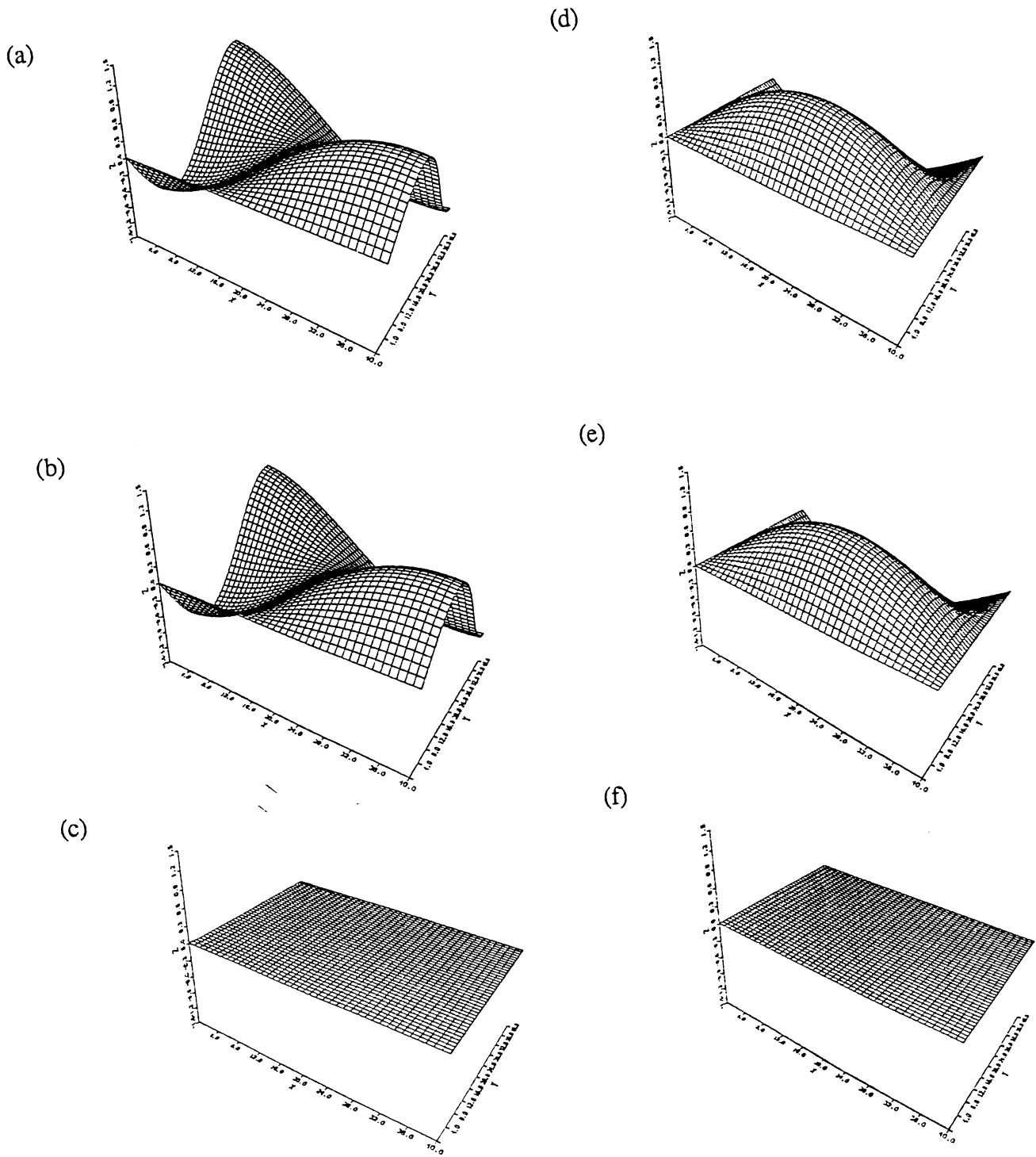


Figure 2.3 Comparison of analytic and numerical results for test examples 1 and 2. Items (a)-(c) show the analytic, numerical and error in the imaginary part of the total field in test example 1. Items (d)-(f) show the analytic, numerical and difference in the real part of the total field in example 2.

where

$$u_2^s(\mathbf{x}) = \begin{cases} c_2 e^{ika_2 \mathbf{x}}, & \mathbf{x} > 0.01 \\ c_3 e^{ik\sqrt{1+a_2^2}\mathbf{x}} + c_4 e^{-ik\sqrt{1+a_2^2}\mathbf{x}} - e^{ika_2 \mathbf{x}}, & |\mathbf{x}| < 0.01 \\ c_1 e^{-ika_2 \mathbf{x}}, & \mathbf{x} < -0.01 \end{cases}$$

$$c_1 = -5.955 \times 10^{-2} + i 0.2305$$

$$c_2 = -5.962 \times 10^{-2} + i 0.2429$$

$$c_3 = 0.8179 + i 0.1167$$

$$c_4 = 9.1789 \times 10^{-2} + i 0.1123$$

The analytic solution and computational solution as well as their difference are plotted in Figure 2.3.

Test Example 2

$$n(\mathbf{x}, z) \equiv 1, \text{ for all } (\mathbf{x}, z)$$

$$u^i(\mathbf{x}, z) = \sin[1.5\pi z] e^{ika_2 \mathbf{x}},$$

$$k = 26.5, a_2 = \sqrt{1 - \frac{1.5^2 \pi^2}{k^2}}.$$

The total solution is $u(\mathbf{x}, z) = u^i(\mathbf{x}, z)$. The plots are shown in Figure 2.3.

Computational Example 1

$$n(\mathbf{x}, z) = \begin{cases} 2, & \mathbf{x}^2 + (z - 0.5)^2 \leq 0.05^2 \\ 1, & \text{elsewhere} \end{cases}$$

$$u^i(\mathbf{x}, z) = \sum_{n=1}^{30} \phi_n(z_0) \phi_n(z) e^{ika_n |\mathbf{x} - \mathbf{x}_0|}, \mathbf{x}_0 = -6000, z_0 = 0.1$$

where $\phi_n(z)$, a_n are the n th eigenfunction and eigenvalue of problem (2.16), (2.17) for $h = 1$, $k = 24$. The near fields of the incident, total and scattered waves are plotted in Figure 2.4.

Scattered Field off Shallow Water Target
 $f = 60$ hz, Target Depth = 55 m, Target Dia. = 10 m
 Source at -30 NM

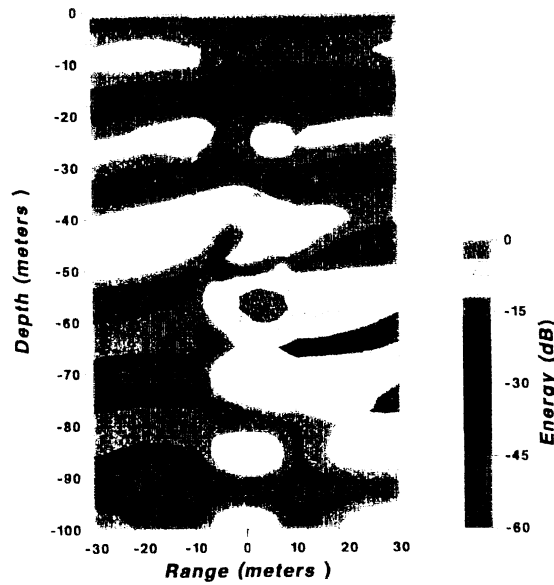


Figure 2.4 Energy in scattered field as described in computational example 1

Computational Example 2

$$n(\mathbf{x}, z) = \begin{cases} 2, & (\mathbf{x} - 0.005)^2 + \frac{(y - .7)^2}{100} \leq 0.01^2 \\ 1, & \text{elsewhere} \end{cases}$$

$$u^i(\mathbf{x}, z) = \phi_4(z)e^{ik_4 \cdot \mathbf{x}}, \quad k = 26.5$$

The near fields of the incident, total and scattered waves are plotted in Figure 2.5.

Computational Example 3

$$n(\mathbf{x}, z) = \begin{cases} 2, & \mathbf{x}^2 + (y - 1)^2 \leq 0.05^2, \quad |\mathbf{x}| \leq 0.02 \\ 1, & \text{elsewhere} \end{cases}$$

$$u^i(\mathbf{x}, z) = \sum_{n=1}^{18} \phi_n(z_0)\phi_n(z)e^{ik_n|\mathbf{x} - \mathbf{x}_0|}, \quad k = 26.5, \quad \mathbf{x}_0 = -5.0, \quad z_0 = 0.025$$

The near fields of the incident, total, and the scattered waves are plotted in Figure 2.6.

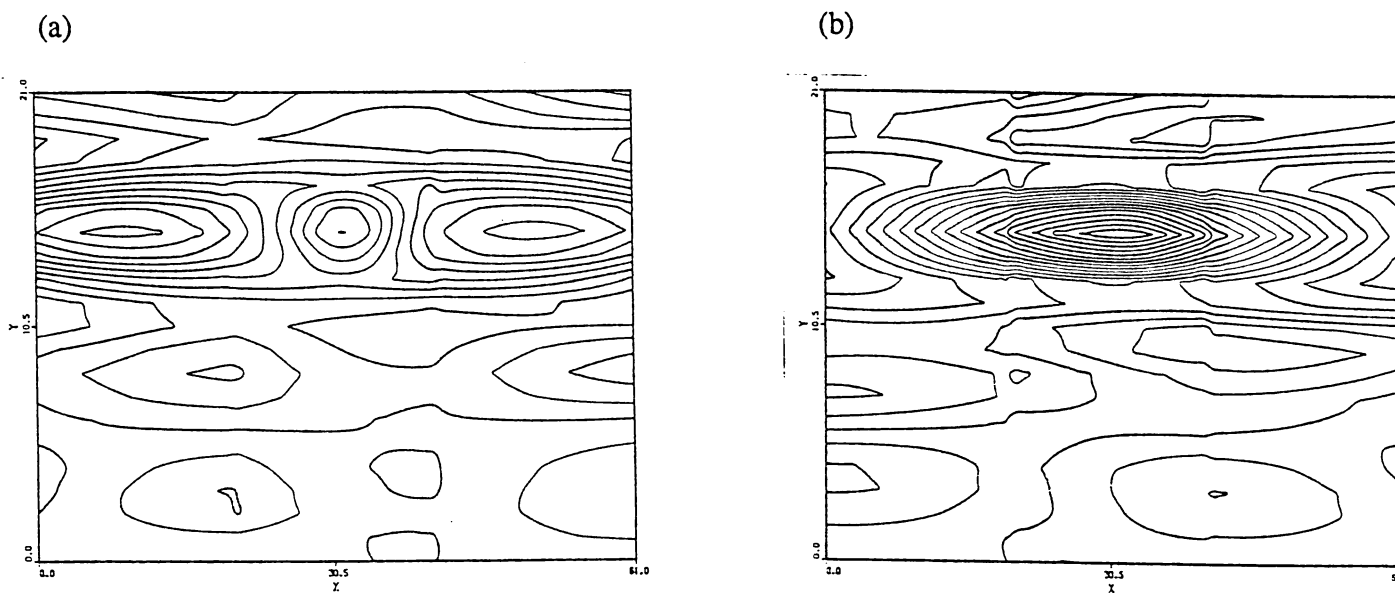


Figure 2.5 Real (Item (a)) and imaginary (Item (b)) parts of scattered field as described in computational example 2.

III. Determination of Inhomogeneity Shape From Scattered Field

3.1 Formulation of the Inverse Problem

Let $G^*(\mathbf{x}, z; \xi, \zeta)$ be the Green's function satisfying the equation

$$\Delta G^* + k^2 n^2(\mathbf{x}, z) G^* = -\delta(\mathbf{x} - \xi) \quad (3.1)$$

with boundary condition

$$G^*(\mathbf{x}, 0; \xi, \zeta) = 0 \quad (3.2)$$

$$\frac{\partial G^*}{\partial z}(\mathbf{x}, h; \xi, \zeta) = 0 \quad (3.3)$$

and outgoing radiation condition as $|\mathbf{x}| \rightarrow \infty$.

Writing

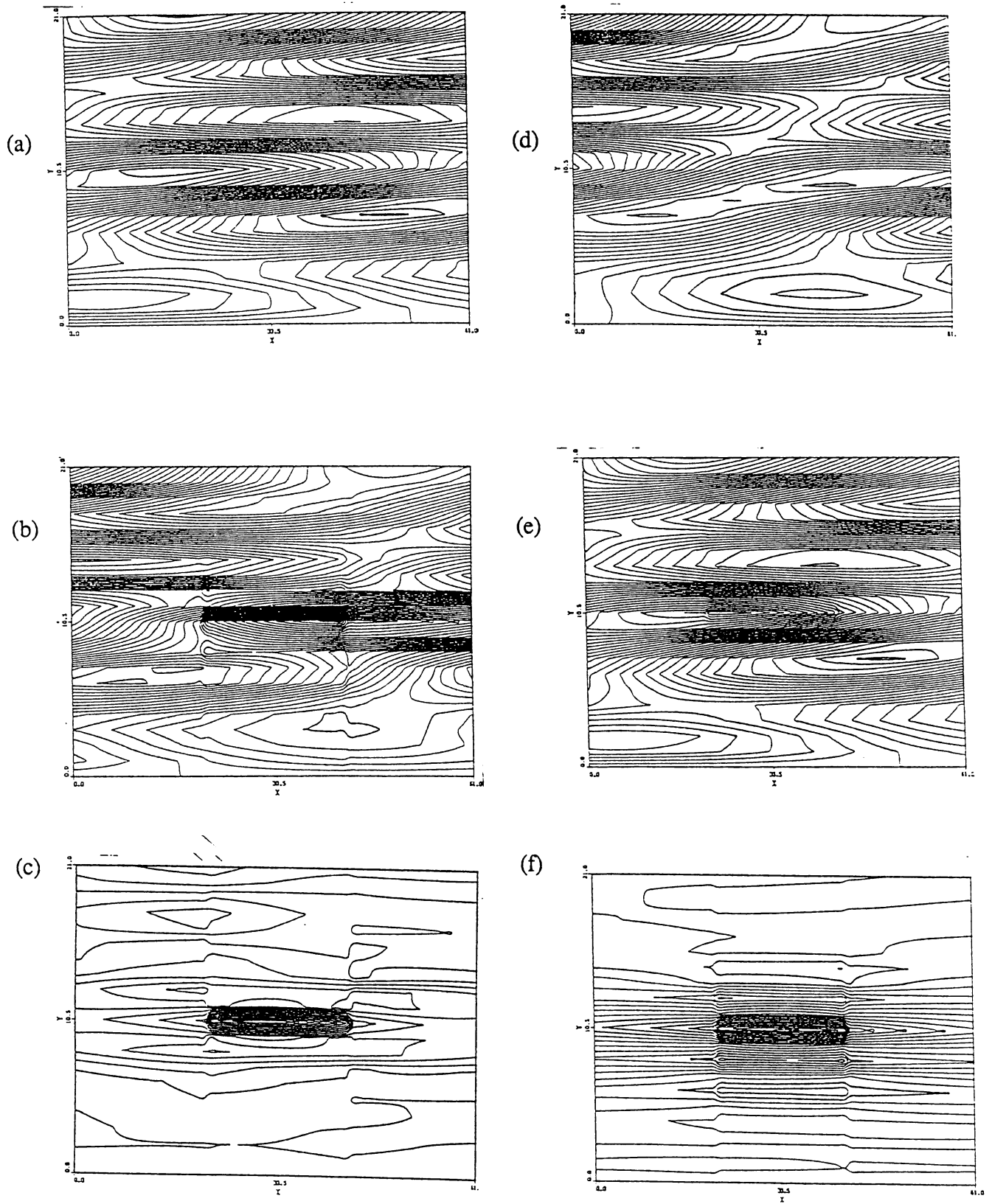


Figure 2.6 Incoming, total and scattered fields in computational example 3. Items (a)-(c) show the real part of the incoming, total and scattered fields, respectively, while items (d)-(f) show the corresponding imaginary parts of the solution.

$$m(\mathbf{x}, z) = n^2(\mathbf{x}, z) - 1, \quad m^*(\mathbf{x}, z) = n_*^2(\mathbf{x}, z) - 1,$$

and rewriting 1.1 in the form

$$\Delta u^s + k^2 n_*^2(\mathbf{x}, z) u^s = k^2 [m_*(\mathbf{x}, z) - m(\mathbf{x}, z)] u^s - k^2 m(\mathbf{x}, z) u^i, \quad (3.4)$$

we obtain the formula

$$u(\mathbf{x}, z) = u_*(\mathbf{x}, z) + k^2 \int_D G^*(\mathbf{x}, z; \xi, \zeta) [m(\xi, \zeta) - m_*(\xi, \zeta)] u(\xi, \zeta) d\xi d\zeta \quad (3.5)$$

where $u_*(\mathbf{x}, z)$ is the total field produced by the wave $u^i(\mathbf{x}, z)$ incident upon the scatterer with the refraction index $n_*(\mathbf{x}, z)$.

i.e.,

$$u_*(\mathbf{x}, z) = u^i(\mathbf{x}, z) + k^2 \int_D G^*(\mathbf{x}, z; \xi, \zeta) n_*(\xi, \zeta) u^i(\xi, \zeta) d\xi d\zeta. \quad (3.6)$$

Since $n_*(\mathbf{x}, z)$ is known, $u_*(\mathbf{x}, z)$ can be produced numerically by the coupled finite element and normal mode methods.

The inverse problem associated with scattering an incident wave $u^i(\mathbf{x}, z)$ by the unknown inhomogeneity now can be formulated according to the measurements made in the near or far-field. For measurements made in the near-field at the set of points $(\mathbf{x}_\ell, z_\ell)$, $\ell = 1, 2, \dots, L$, we obtain from (3.5) the relations

$$k^2 \int_D G^*(\mathbf{x}_\ell, z_\ell; \xi, \zeta) [m(\xi, \zeta) - m_*(\xi, \zeta)] u(\xi, \zeta) d\xi d\zeta = b_\ell, \quad (3.7)$$

where b_ℓ is the complex number corresponding to the difference in the measured value of $u(\mathbf{x}_\ell, z_\ell)$ and the calculated value of $u_*(\mathbf{x}_\ell, z_\ell)$:

$$b_\ell = u(\mathbf{x}_\ell, z_\ell) - u_*(\mathbf{x}_\ell, z_\ell) \quad (3.8)$$

Next consider the case when measurements are made in the far-field. The asymptotic form of $G^*(\mathbf{x}, z; \xi, \zeta)$ as $|\mathbf{x}| \rightarrow \infty$ is needed. Decompose the Green's function $G^*(\mathbf{x}, z; \xi, \zeta)$ in the form

$$G^*(\mathbf{x}, z; \xi, \zeta) = G(\mathbf{x}, z; \xi, \zeta) + \tilde{G}(\mathbf{x}, z; \xi, \zeta), \quad (3.9)$$

where

$$G(\mathbf{x}, z; \xi, \zeta) = \frac{2}{h} \sum_{n=1}^{\infty} \sin \left[\left(n - \frac{1}{2} \right) \frac{\pi z}{h} \right] \sin \left[\left(n - \frac{1}{2} \right) \frac{\pi \zeta}{h} \right] e^{ika_n |\mathbf{x} - \xi|},$$

$$a_n = \left[1 - \left(n - \frac{1}{2} \right)^2 \frac{\pi^2}{k^2 h^2} \right]^{\frac{1}{2}}, \quad (3.10)$$

observe that $\tilde{G}(\mathbf{x}, z; \xi, \zeta)$ is continuous on (\mathbf{x}, z) and (ξ, ζ) since it satisfies the integral equation

$$\begin{aligned} \tilde{G}(\mathbf{x}, z; \xi, \zeta) &= k^2 \int_{\mathcal{D}} G(\mathbf{x}, z; \hat{\xi}, \hat{\zeta}) G(\hat{\xi}, \hat{\zeta}; \xi, \zeta) m_*(\hat{\xi}, \hat{\zeta}) d\hat{\xi} d\hat{\zeta} \\ &+ k^2 \int_{\mathcal{D}} G(\mathbf{x}, z; \hat{\xi}, \hat{\zeta}) \tilde{G}(\hat{\xi}, \hat{\zeta}; \xi, \zeta) m_*(\hat{\xi}, \hat{\zeta}) d\hat{\xi} d\hat{\zeta} \end{aligned} \quad (3.11)$$

Since a_n is purely imaginary as $n > N := \left[\frac{1}{2} + \frac{kh}{\pi} \right]$, $G(\mathbf{x}, z; \xi, \zeta)$ has the asymptotic form

$$G(\mathbf{x}, z; \xi, \zeta) = \frac{2}{h} \sum_{n=1}^N \sin \left[\left(n - \frac{1}{2} \right) \frac{\pi z}{h} \right] \sin \left[\left(n - \frac{1}{2} \right) \frac{\pi \zeta}{h} \right] e^{-ika_n \frac{\mathbf{x}}{|\mathbf{x}|} \xi} e^{ika_n |\mathbf{x}|} + O \left(\frac{1}{|\mathbf{x}|} \right), \quad \text{as } |\mathbf{x}| \rightarrow \infty. \quad (3.12)$$

Hence, $\tilde{G}(\mathbf{x}, z; \xi, \zeta)$ has the asymptotic form

$$\tilde{G}(\mathbf{x}, z; \xi, \zeta) = \frac{2}{h} \sum_{n=1}^N \sin \left[\left(n - \frac{1}{2} \right) \frac{\pi z}{h} \right] e^{ika_n |\mathbf{x}|} \tilde{f}_n \left(\frac{\mathbf{x}}{|\mathbf{x}|} \right) + O \left(\frac{1}{|\mathbf{x}|} \right), \quad (3.13)$$

where

$$\tilde{f}_n \left(\frac{\mathbf{x}}{|\mathbf{x}|} \right) = \int_{\mathcal{D}} \sin \left[\left(n - \frac{1}{2} \right) \frac{\pi \hat{\zeta}}{h} \right] e^{-ika_n \frac{\mathbf{x}}{|\mathbf{x}|} \hat{\xi}} G^*(\hat{\xi}, \hat{\zeta}; \xi, \zeta) m_*(\hat{\xi}, \hat{\zeta}) d\hat{\xi} d\hat{\zeta},$$

and $G^*(\hat{\xi}, \hat{\zeta}; \xi, \zeta)$ has the asymptotic form

$$G^*(\mathbf{x}, z; \xi, \zeta) = \frac{2}{h} \sum_{n=1}^N \sin \left[\left(n - \frac{1}{2} \right) \frac{\pi z}{h} \right] e^{ika_n |\mathbf{x}|} \tilde{f}_n^* \left(\frac{\mathbf{x}}{|\mathbf{x}|} \right) + O \left(\frac{1}{|\mathbf{x}|} \right), \quad \text{as } |\mathbf{x}| \rightarrow \infty \quad (3.14)$$

where

$$\mathbf{f}_n^*\left(\frac{\mathbf{x}}{|\mathbf{x}|}\right) = \sin\left[\left(n - \frac{1}{2}\right)\frac{\pi\zeta}{h}\right] e^{-ika_n\frac{\mathbf{x}}{|\mathbf{x}|\zeta}} + \tilde{\mathbf{f}}_n\left(\frac{\mathbf{x}}{|\mathbf{x}|}\right).$$

From (3.6) and (3.5)

$$\mathbf{u}^s(\mathbf{x}, z) = \frac{2}{h} \sum_{n=1}^N \sin\left[\left(n - \frac{1}{2}\right)\frac{\pi z}{h}\right] e^{ika_n|\mathbf{x}|} \left\{ \left(\mathbf{f}_n^*\left(\frac{\mathbf{x}}{|\mathbf{x}|}\right), \mathbf{k}^2 \mathbf{n}_* \mathbf{u}^i \right) + \left(\mathbf{f}_n^*\left(\frac{\mathbf{x}}{|\mathbf{x}|}\right), \mathbf{k}^2 (\mathbf{m} - \mathbf{m}_*) \mathbf{u} \right) \right\} + O\left(\frac{1}{|\mathbf{x}|}\right),$$

as $|\mathbf{x}| \rightarrow \infty$ (3.15)

where (\cdot, \cdot) is the integral over D.

The vector

$$\mathbf{F}\left(\frac{|\mathbf{x}|}{\mathbf{x}}, z\right) := \left(\mathbf{f}_1\left(\frac{|\mathbf{x}|}{\mathbf{x}}\right) \phi_1(z), \mathbf{f}_2\left(\frac{|\mathbf{x}|}{\mathbf{x}}\right) \phi_2(z), \dots, \mathbf{f}_n\left(\frac{|\mathbf{x}|}{\mathbf{x}}\right) \phi_n(z) \right),$$

where

$$\phi_n(z) = \frac{2}{h} \sin\left[\left(n - \frac{1}{2}\right)\frac{\pi z}{h}\right],$$

$$\mathbf{f}_n\left(\frac{|\mathbf{x}|}{\mathbf{x}}\right) = \left(\mathbf{f}_n^*\left(\frac{|\mathbf{x}|}{\mathbf{x}}\right), \mathbf{k}^2 \mathbf{n}_* \mathbf{u}^i + \mathbf{k}^2 (\mathbf{m} - \mathbf{m}_*) \mathbf{u} \right),$$

is called the propagating far-field pattern of the scattered field $\mathbf{u}^s(\mathbf{x}, z)$ (cf. [4]).

For measurements made in the far-field in the direction $\mathbf{x} > 0$ or $\mathbf{x} < 0$ for $z \in [0, h]$, we can obtain from (3.15) the relations

$$\mathbf{k}^2 \int_D \mathbf{f}_n^*\left(\frac{\mathbf{x}}{|\mathbf{x}|}, \zeta\right) \left[\mathbf{m}(\xi, \zeta) - \mathbf{m}_*(\xi, \zeta) \right] \mathbf{u}(\xi, \zeta) d\xi d\zeta = \mathbf{b}_n\left(\frac{\mathbf{x}}{|\mathbf{x}|}\right), \quad n = 1, 2, \dots, N. \quad (3.16)$$

Here N is the number of propagating modes and \mathbf{b}_n is the coefficient of the n th normal mode of the difference between the measured data and the calculated far-field associated with index of refraction $\mathbf{n}_*(\mathbf{x}, z)$:

i.e.,

$$\mathbf{b}_n\left(\frac{\mathbf{x}}{|\mathbf{x}|}\right) = \int_0^h \frac{2}{h} \sin\left[\left(n - \frac{1}{2}\right)\frac{\pi z}{h}\right] \left[\mathbf{u}^s(\mathbf{x}, z) e^{-ika_n|\mathbf{x}|} \right] dz - \left(\mathbf{f}_n^*\left(\frac{\mathbf{x}}{|\mathbf{x}|}\right), \mathbf{k}^2 \mathbf{n}_* \mathbf{u}^i \right). \quad (3.17)$$

Observe that the inverse problem based on far-field measurement has a particular difficulty caused by the fact that only a finite number of modes can propagate. This loss of information cannot be recovered by mathematical procedure. Some a priori knowledge of the refraction index is crucial for the purpose of recovering the obstacle shape. Discussions of this problem can be found in [3].

The inverse problem we consider in this paper can be stated as follows:

- (1) Near field measurement: find the real continuous function $m(\mathbf{x}, z)$ vanishing on the boundary of D such that (3.7) and (3.5) are satisfied.
- (2) Far-field measurement: find the real continuous function $m(\mathbf{x}, z)$ vanishing on the boundary of D such that (3.15) and (3.5) are satisfied.

In this paper we will present only the numerical results for the inverse problem from near-field measurement. The obstacle shape determination from far-field measurement is discussed by Gilbert and Xu [4] using a Colton-Monk type method [6]. The result for Problem 2 will be presented in a separate paper.

3.2 Minimization Algorithm for Solution of the Linear Functional Equations.

The inhomogeneity shape is determined by solving for $m(\xi, \zeta)$ in (3.7). Since $u(\xi, \zeta)$ is a function of $n(\xi, \zeta) = 1 + m(\xi, \zeta)$, (3.7) is a nonlinear equation of $m(\xi, \zeta)$. Following Weston, we simplify the problem by introducing a function

$$w = (m - m_*)u$$

and consider the linearized equations

$$Gw(\mathbf{x}_\ell, z_\ell) := k^2 \int_D G^*(\mathbf{x}_\ell, z_\ell; \xi, \zeta) w(\xi, \zeta) d\xi d\zeta = b_\ell \quad (3.18)$$

with constraints (cf. [5]).

$$\text{Im } \overline{w} [u_* + Gw] = 0 \quad (3.19)$$

$$\frac{|u_* + Gw|}{|w|} \geq c > 0 \quad \text{for some constant } c. \quad (3.20)$$

The inhomogeneity is given through

$$m - m_* = \frac{w}{[u_* + Gw]}. \quad (3.21)$$

In this paper, we present a minimization algorithm to approximate the solution w .

Define the functional

$$J(\mathbf{w}) = \sum_{\ell=1}^L \left| \mathbf{k}^2 \int_D G^*(\mathbf{x}_\ell, \mathbf{z}_\ell; \xi, \zeta) \mathbf{w}(\xi, \zeta) d\xi d\zeta - \mathbf{b}_\ell \right|^2 + \left\| \text{Im } \overline{\mathbf{w}} [\mathbf{u}_* + G\mathbf{w}] \right\|_{L^2(D)}. \quad (3.22)$$

and solve for the minimizer \mathbf{w}^*

$$J(\mathbf{w}^*) = \min_{\mathbf{w} \in C(M)} J(\mathbf{w}) \quad (3.23)$$

where

$$C(M) = \{u \mid u \text{ is continuous in } D, |u| \leq M, u|_{\partial D} = 0\},$$

M is a positive constant. It is clear that if $M = \infty$, then $J(\mathbf{w}^*) = 0$. (\mathbf{w}^* may not be unique.)

Let

$$\overline{\mathbf{w}} \mathbf{u}_* = \phi(\mathbf{x}, \mathbf{z}) - i\psi(\mathbf{x}, \mathbf{z}), \quad (3.24)$$

(3.21) implies

$$J(\phi, \psi) = \sum_{\ell=1}^L \left| V(\phi + i\psi)(\mathbf{x}_\ell, \mathbf{z}_\ell) - \mathbf{b}_\ell \right|^2 + \left\| (\psi, \phi) \mathbb{W} \begin{pmatrix} \psi \\ \phi \end{pmatrix} - \psi \right\|_{L^2(D)} \quad (3.25)$$

where

$$\mathbb{W} = \begin{pmatrix} L_I & -L_R \\ L_R & L_I \end{pmatrix}$$

and

$$L_I f := \mathbf{k}^2 \int_D (\text{Im } G^*) [\mathbf{u}_*(\mathbf{x}, \mathbf{z}) \overline{\mathbf{u}}_*(\xi, \zeta)]^{-1} f d\xi d\zeta \quad (3.26)$$

$$L_R f := \mathbf{k}^2 \int_D (\text{Re } G^*) [\mathbf{u}_*(\mathbf{x}, \mathbf{z}) \overline{\mathbf{u}}_*(\xi, \zeta)]^{-1} f d\xi d\zeta \quad (3.27)$$

$$V(\phi + i\psi)(\mathbf{x}_\ell, \mathbf{z}_\ell) := \mathbf{k}^2 \int_D G^*(\mathbf{x}_\ell, \mathbf{z}_\ell; \xi, \zeta) \overline{\mathbf{u}}^{-1}(\xi, \zeta) [\phi(\xi, \zeta) + i\psi(\xi, \zeta)] d\xi d\zeta. \quad (3.28)$$

We assume it is known that the inhomogeneity is contained in a box $D = [-\mathbf{d}, \mathbf{d}] \times [\mathbf{h}_1, \mathbf{h}_2]$. A pair of functions (ψ, ϕ) is approximated by

$$\psi_{kj}(\mathbf{x}, z) = \sum_{k=1}^K \sum_{j=1}^J \alpha_{kj} \sin \frac{k\pi(\mathbf{x} + d)}{2d} \sin \frac{j\pi(z - h_1)}{h_2 - h_1},$$

$$\phi_{kj}(\mathbf{x}, z) = \sum_{k=1}^K \sum_{j=1}^J \beta_{kj} \sin \frac{k\pi(\mathbf{x} + d)}{2d} \sin \frac{j\pi(z - h_1)}{h_2 - h_1}.$$

The discretization of $J(\phi, \psi)$ gives a quadratic function of $\alpha_{k,j}$, $\beta_{k,j}$. A minimization subroutine is then used to produce $\alpha_{k,j}$, $\beta_{k,j}$. Finally, from (3.21) the refraction index $n(\mathbf{x}, z)$ is recovered by

$$n(\mathbf{x}, z) = 1 + m_*(\mathbf{x}, z) + \frac{1}{|u_*|^2} \phi[1 + L_R \phi - L_I \psi]^{-1}.$$

The convergence of this algorithm will be presented in a separate paper. The numerical result will be presented at this conference.

Acknowledgements

The authors would like to thank Professor Peter Monk for allowing them to modify his finite element program for their application.

References

- [1] Colton, D., R. Ewing and W. Rundell, Inverse Problems in Partial Differential Equations, SIAM, Philadelphia, 1990.
- [2] Kirsch, A. and P. Monk, "Convergence Analysis of a Coupled Finite Element and Spectral Method in Acoustic Scattering", IMA J. Numerical Analysis (1990) 9, 425-447.
- [3] Xu, Y. "An Injective Far-field Pattern Operator and Inverse Scattering Problem in a Finite Depth Ocean", Proc. Edinburgh Math Society (1991). (to appear)
- [4] Gilbert, R. and Y. Xu, "Generalized Herglotz Functions and Inverse Scattering Problem in a Finite Depth Ocean", SIAM Proc. (1991). (to appear)
- [5] Weston, V., "Inverse Problem for the Reduced Wave Equation With Fixed Incident Field", J. Math. Phys. 21 (4), April 1980; 22 (11) Nov. 1981.
- [6] Colton, D. and P. Monk, "A Novel Method for Solving the Inverse Scattering Problem for Time-harmonic Acoustic Waves in the Resonance Region", SIAM J. Appl. Math. 46, 506-523 (1986).

Recent IMA Preprints

#	Author/s	Title
746	Chris Grant,	Solutions to evolution equations with near-equilibrium initial values
747	Mario Taboada and Yuncheng You,	Invariant manifolds for retarded semilinear wave equations
748	Peter Rejto and Mario Taboada,	Unique solvability of nonlinear Volterra equations in weighted spaces
749	Hi Jun Choe,	Holder regularity for the gradient of solutions of certain singular parabolic equations
750	Jack D. Dockery,	Existence of standing pulse solutions for an excitable activator-inhibitory system
751	Jack D. Dockery and Roger Lui,	Existence of travelling wave solutions for a bistable evolutionary ecology model
752	Giovanni Alberti, Luigi Ambrosio and Giuseppe Buttazzo,	Singular perturbation problems with a compact support semilinear term
753	Emad A. Fatemi,	Numerical schemes for constrained minimization problems
754	Y. Kuang and H.L. Smith,	Slowly oscillating periodic solutions of autonomous state-dependent delay equations
755	Emad A. Fatemi,	A new splitting method for scalar conservation laws with stiff source terms
756	Hi Jun Choe,	A regularity theory for a more general class of quasilinear parabolic partial differential equations and variational inequalities
757	Haitao Fan,	A vanishing viscosity approach on the dynamics of phase transitions in Van Der Waals fluids
758	T.A. Osborn and F.H. Molzahn,	The Wigner–Weyl transform on tori and connected graph propagator representations
759	Avner Friedman and Bei Hu,	A free boundary problem arising in superconductor modeling
760	Avner Friedman and Wenxiong Liu,	An augmented drift-diffusion model in semiconductor device
761	Avner Friedman and Miguel A. Herrero,	Extinction and positivity for a system of semilinear parabolic variational inequalities
762	David Dobson and Avner Friedman,	The time-harmonic Maxwell equations in a doubly periodic structure
763	Hi Jun Choe,	Interior behaviour of minimizers for certain functionals with nonstandard growth
764	Vincenzo M. Tortorelli and Epifanio G. Virga,	Axis-symmetric boundary-value problems for nematic liquid crystals with variable degree of orientation
765	Nikan B. Firoozye and Robert V. Kohn,	Geometric parameters and the relaxation of multiwell energies
766	Haitao Fan and Marshall Slemrod,	The Riemann problem for systems of conservation laws of mixed type
767	Joseph D. Fehribach,	Analysis and application of a continuation method for a self-similar coupled Stefan system
768	C. Foias, M.S. Jolly, I.G. Kevrekidis and E.S. Titi,	Dissipativity of numerical schemes
769	D.D. Joseph, T.Y.J. Liao and J.-C. Saut,	Kelvin–Helmholtz mechanism for side branching in the displacement of light with heavy fluid under gravity
770	Chris Grant,	Solutions to evolution equations with near-equilibrium initial values
771	B. Cockburn, F. Coquel, Ph. LeFloch and C.W. Shu,	Convergence of finite volume methods
772	N.G. Lloyd and J.M. Pearson,	Computing centre conditions for certain cubic systems
773	João Palhoto Matos,	Young measures and the absence of fine microstructures in the $\alpha - \beta$ quartz phase transition
774	L.A. Peletier & W.C. Troy,	Self-similar solutions for infiltration of dopant into semiconductors
775	H. Scott Dumas and James A. Ellison,	Nekhoroshev’s theorem, ergodicity, and the motion of energetic charged particles in crystals
776	Stathis Filippas and Robert V. Kohn,	Refined asymptotics for the blowup of $u_t - \Delta u = u^p$.
777	Patricia Bauman, Nicholas C. Owen and Daniel Phillips,	Maximum principles and a priori estimates for an incompressible material in nonlinear elasticity
778	Patricia Bauman, Nicholas C. Owen and Daniel Phillips,	Maximal smoothness of solutions to certain Euler–Lagrange equations from nonlinear elasticity
779	Jack Carr and Robert Pego,	Self-similarity in a coarsening model in one dimension
780	J.M. Greenberg,	The shock generation problem for a discrete gas with short range repulsive forces
781	George R. Sell and Mario Taboada,	Local dissipativity and attractors for the Kuramoto–Sivashinsky equation in thin 2D domains
782	T. Subba Rao,	Analysis of nonlinear time series (and chaos) by bispectral methods
783	Nicholas Baumann, Daniel D. Joseph, Paul Mohr and Yuriko Renardy,	Vortex rings of one fluid in another free fall
784	Oscar Bruno, Avner Friedman and Fernando Reitich,	Asymptotic behavior for a coalescence problem
785	Johannes C.C. Nitsche,	Periodic surfaces which are extremal for energy functionals containing curvature functions
786	F. Abergel and J.L. Bona,	A mathematical theory for viscous, free-surface flows over a perturbed plane
787	Gunduz Caginalp and Xinfu Chen,	Phase field equations in the singular limit of sharp interface problems
788	Robert P. Gilbert and Yongzhi Xu,	An inverse problem for harmonic acoustics in stratified oceans
789	Roger Fosdick and Eric Volkmann,	Normality and convexity of the yield surface in nonlinear plasticity
790	H.S. Brown, I.G. Kevrekidis and M.S. Jolly,	A minimal model for spatio-temporal patterns in thin film flow

- 791 **Chao–Nien Chen**, On the uniqueness of solutions of some second order differential equations
- 792 **Xinfu Chen and Avner Friedman**, The thermistor problem for conductivity which vanishes at large temperature
- 793 **Xinfu Chen and Avner Friedman**, The thermistor problem with one-zero conductivity
- 794 **E.G. Kalnins and W. Miller, Jr.**, Separation of variables for the Dirac equation in Kerr Newman space time
- 795 **E. Knobloch, M.R.E. Proctor and N.O. Weiss**, Finite-dimensional description of doubly diffusive convection
- 796 **V.V. Pukhnachov**, Mathematical model of natural convection under low gravity
- 797 **M.C. Knaap**, Existence and non-existence for quasi-linear elliptic equations with the p-laplacian involving critical Sobolev exponents
- 798 **Stathis Filippas and Wenxiong Liu**, On the blowup of multidimensional semilinear heat equations
- 799 **A.M. Meirmanov**, The Stefan problem with surface tension in the three dimensional case with spherical symmetry: non-existence of the classical solution
- 800 **Bo Guan and Joel Spruck**, Interior gradient estimates for solutions of prescribed curvature equations of parabolic type
- 801 **Hi Jun Choe**, Regularity for solutions of nonlinear variational inequalities with gradient constraints
- 802 **Peter Shi and Yongzhi Xu**, Quasistatic linear thermoelasticity on the unit disk
- 803 **Satyanad Kichenassamy and Peter J. Olver**, Existence and non-existence of solitary wave solutions to higher order model evolution equations
- 804 **Dening Li**, Regularity of solutions for a two-phase degenerate Stefan Problem
- 805 **Marek Fila, Bernhard Kawohl and Howard A. Levine**, Quenching for quasilinear equations
- 806 **Yoshikazu Giga, Shun'ichi Goto and Hitoshi Ishii**, Global existence of weak solutions for interface equations coupled with diffusion equations
- 807 **Mark J. Friedman and Eusebius J. Doedel**, Computational methods for global analysis of homoclinic and heteroclinic orbits: a case study
- 808 **Mark J. Friedman**, Numerical analysis and accurate computation of heteroclinic orbits in the case of center manifolds
- 809 **Peter W. Bates and Songmu Zheng**, Inertial manifolds and inertial sets for the phase-field equations
- 810 **J. López Gómez, V. Márquez and N. Wolanski**, Global behavior of positive solutions to a semilinear equation with a nonlinear flux condition
- 811 **Xinfu Chen and Fahuai Yi**, Regularity of the free boundary of a continuous casting problem
- 812 **Eden, A., Foias, C., Nicolaenko, B. and Temam, R.**, Inertial sets for dissipative evolution equations Part I: Construction and applications
- 813 **Jose–Francisco Rodrigues and Boris Zaltzman**, On classical solutions of the two-phase steady-state Stefan problem in strips
- 814 **Viorel Barbu and Srdjan Stojanovic**, Controlling the free boundary of elliptic variational inequalities on a variable domain
- 815 **Viorel Barbu and Srdjan Stojanovic**, A variational approach to a free boundary problem arising in electrophotography
- 816 **B.H. Gilding and R. Kersner**, Diffusion-convection-reaction, free boundaries, and an integral equation
- 817 **Shoshana Kamin, Lambertus A. Peletier and Juan Luis Vazquez**, On the Barenblatt equation of elastoplastic filtration
- 818 **Avner Friedman and Bei Hu**, The Stefan problem with kinetic condition at the free boundary
- 819 **M.A. Grinfeld**, The stress driven instabilities in crystals: mathematical models and physical manifestations
- 820 **Bei Hu and Lihe Wang**, A free boundary problem arising in electrophotography: solutions with connected toner region
- 821 **Yongzhi Xu, T. Craig Poling, and Trent Brundage**, Direct and inverse scattering of time harmonic acoustic waves in an inhomogeneous shallow ocean
- 822 **Steven J. Altschuler**, Singularities of the curve shrinking flow for space curves
- 823 **Steven J. Altschuler and Matthew A. Grayson**, Shortening space curves and flow through singularities
- 824 **Tong Li**, On the Riemann problem of a combustion model
- 825 **L.A. Peletier & W.C. Troy**, Self-similar solutions for diffusion in semiconductors
- 826 **C.J. van Duijn, L.A. Peletier & R.J. Schotting**, On the analysis of brine transport in porous media
- 827 **Minkyu Kwak**, Finite dimensional description of convective reaction-diffusion equations
- 828 **Minkyu Kwak**, Finite dimensional inertial forms for the 2D Navier–Stokes equations
- 829 **Victor A. Galaktionov and Sergey A. Posashkov**, On some monotonicity in time properties for a quasilinear parabolic equation with source
- 830 **Victor A. Galaktionov**, Remark on the fast diffusion equation in a ball
- 831 **Hi Jun Choe and Lihe Wang**, A regularity theory for degenerate vector valued variational inequalities
- 832 **Vladimir I. Olikier and Nina N. Uraltseva**, Evolution of nonparametric surfaces with speed depending on curvature, II. The mean curvature case.
- 833 **S. Kamin and W. Liu**, Large time behavior of a nonlinear diffusion equation with a source
- 834 **Shoshana Kamin and Juan Luis Vazquez**, Singular solutions of some nonlinear parabolic equations
- 835 **Bernhard Kawohl and Robert Kersner**, On degenerate diffusion with very strong absorption